

# Large System Analysis of Box-Relaxation in Correlated Massive MIMO Channels Under Imperfect CSI (Extended Version)

Ayed M. Alrashdi

Email: am.alrashdi@uoh.edu.sa

## Abstract

In this paper, we study the mean square error (MSE) and the bit error rate (BER) performance of the box-relaxation decoder in massive multiple-input-multiple-output (MIMO) systems under the assumptions of imperfect channel state information (CSI) and receive-side channel correlation. Our analysis assumes that the number of transmit and receive antennas ( $n$  and  $m$ ) grow simultaneously large while their ratio remains fixed. For simplicity of the analysis, we consider binary phase shift keying (BPSK) modulated signals. The asymptotic approximations of the MSE and BER enable us to derive the optimal power allocation scheme under MSE/BER minimization. Numerical simulations suggest that the asymptotic approximations are accurate even for small  $n$  and  $m$ . They also show the important role of the box constraint in mitigating the so called double descent phenomenon.

## Index Terms

Asymptotic analysis, CGMT, box relaxation, channel correlation, channel estimation, power allocation.

## I. INTRODUCTION

Massive multiple-input multiple-output (MIMO) is considered one of the key enabling technologies for the future cellular networks as it promises significant gains in data rates, spectral and energy efficiency, and link reliability [1]–[6]. The idea of massive MIMO is to use a large number of antennas at the base station to serve many users at the same time and frequency resources. To attain the significant benefits

The author is with the Department of Electrical Engineering, College of Engineering, University of Ha'il, P.O. Box 2440, Ha'il, 81441, Saudi Arabia (e-mail: am.alrashdi@uoh.edu.sa). This work was supported by the University of Ha'il, Saudi Arabia.

of massive MIMO, accurate knowledge of the channel state information (CSI) is required. A popular approach for acquiring CSI is through training by sending a known sequence of pilot symbols. Thus, prior knowledge of the transmitted pilot sequence is directly incorporated in the process of estimating the CSI. Following this step, the receiver employs the estimated CSI to detect the corresponding transmitted data symbols.

The quality of the recovered symbols can be improved by controlling the power allocation between the transmitted pilot sequences and data symbols to meet specific optimization criteria. Different metrics have been proposed for the power allocation optimization starting from maximizing the channel capacity [7]–[9], maximizing the sum rates [10]–[12], minimizing the mean square error (MSE) [13], [14] or minimization of the bit error rate (BER) and symbol error rate (SER) [15]–[17], and many other metrics depending on the specific application.

The power allocation in the aforementioned works was considered mainly for uncorrelated channel models. In practice, wireless communication systems, including massive MIMO systems, are generally spatially correlated [18]. The power optimization problem was developed for correlated channels to maximize the sum rates [19], [20], or the spectral efficiency [21], [22].

In this work, we propose the use of the box-relaxation optimization (BRO) [23]–[25] as a low complexity decoder for a spatially correlated massive MIMO system. First, we derive novel precise asymptotic approximations of its MSE and BER performance using binary phase shift keying (BPSK) signaling for simplicity. Then, these approximations are used to derive the optimal power allocation scheme. The essential technical tool used in our analysis is the recently developed convex Gaussian min-max theorem (CGMT) [26], [27].

The CGMT framework has been used to analyze the error performance of many problems under independent and identically distributed (iid) assumption on the entries of the channel matrix [26]–[32]. Furthermore, for correlated channel matrices, the CGMT was recently used in [33], [34] to analyze the BRO and the LASSO decoders, respectively. However, these references assume the ideal scenario of perfect knowledge of the CSI matrix. At the same time, this work tackles the more practical and challenging case of imperfect CSI under correlated channel matrix.

The remainder of this paper is organized as follows. Section II describes the considered system model. The asymptotic analysis and optimal power allocation are presented in Section III. Section IV presents the numerical simulations that show the high accuracy of the proposed theoretical results. A proof outline of the main results is given in Section V. Finally, the paper is concluded in Section VI.

## II. SYSTEM MODEL

We consider a flat block-fading massive MIMO system with  $n$  transmitters and  $m$  receivers. The channel between the transmit and receive antennas is modeled as [35], [36]

$$\mathbf{A} = \mathbf{R}^{1/2} \mathbf{H}, \quad (1)$$

where  $\mathbf{R} \in \mathbb{R}^{m \times m}$  is known Hermitian positive semi-definite spatial correlation matrix which models the correlation among the receive side antennas,<sup>1</sup> while  $\mathbf{H} \in \mathbb{R}^{m \times n}$  is a Gaussian matrix with iid entries  $\mathcal{N}(0, 1)$  that represents Rayleigh fast-fading channel. Using this block fading model, each channel coherence interval of length  $T$  is split into two phases starting by training and followed with data transmission. In the training interval of  $T_p \geq n$  symbols, orthogonal sequences of known pilot symbols with average power  $\rho_p$  are transmitted which allows to estimate the channel. The remaining phase is devoted for transmitting  $T_d = T - T_p$  data symbols with average power  $\rho_d$ .

Conservation of time and energy implies that:  $\rho_p T_p + \rho_d T_d = \rho T$ , where  $\rho$  is the expected average power. Alternatively, we can write  $\rho_d T_d = \alpha \rho T$ , where  $\alpha \in [0, 1]$  is the ratio of the power allocated to the data, and then  $\rho_p T_p = (1 - \alpha) \rho T$  is the energy of the pilots. The received signal  $\mathbf{y} \in \mathbb{R}^m$  model for the *data* transmission phase is given by

$$\mathbf{y} = \sqrt{\frac{\rho_d}{n}} \mathbf{A} \mathbf{x}_0 + \mathbf{z}, \quad (2)$$

where  $\mathbf{x}_0 \in \{\pm 1\}^n$  is a BPSK signal,  $\mathbf{A} \in \mathbb{R}^{m \times n}$  is the MIMO channel given in (1), and  $\mathbf{z} \in \mathbb{R}^m$  is the noise vector that has iid entries  $\mathcal{N}(0, 1)$ .

### A. Channel Estimation

The channel matrix  $\mathbf{A}$  needs to be estimated prior to decoding the received data signal. Letting  $\widehat{\mathbf{A}}$  to denote the estimate of the channel matrix, in this work, we consider linear minimum mean square error (LMMSE) estimate which is given by [37]

$$\widehat{\mathbf{A}} = \sqrt{\frac{n}{\rho_p}} \mathbf{R} \left( \mathbf{R} + \frac{n}{T_p \rho_p} \mathbf{I}_m \right)^{-1} \mathbf{Y}_p \mathbf{X}_p^\top, \quad (3)$$

where  $\mathbf{Y}_p = \sqrt{\frac{\rho_p}{n}} \mathbf{A} \mathbf{X}_p + \mathbf{Z}_p \in \mathbb{R}^{m \times T_p}$  is the received signal corresponding to the *training* phase,  $\mathbf{X}_p \in \mathbb{R}^{n \times T_p}$  is the matrix of transmitted orthogonal pilot symbols, and  $\mathbf{Z}_p \in \mathbb{R}^{m \times T_p}$  is an additive white Gaussian noise (AWGN) matrix with  $\mathbb{E}[\mathbf{Z}_p \mathbf{Z}_p^\top] = T_p \mathbf{I}_m$ . According to [21], [37], the  $k^{\text{th}}$  column (for all  $k \leq n$ ) of  $\widehat{\mathbf{A}}$  is distributed as  $\mathcal{N}(\mathbf{0}, \mathbf{R}_{\widehat{\mathbf{A}}})$  with a covariance matrix  $\mathbf{R}_{\widehat{\mathbf{A}}}$  that is given by  $\mathbf{R}_{\widehat{\mathbf{A}}} = \mathbf{R} \left( \mathbf{R} + \frac{n}{T_p \rho_p} \mathbf{I}_m \right)^{-1} \mathbf{R}$ .

<sup>1</sup>For analysis purpose, we assume that  $\mathbf{R}$  satisfies  $\frac{1}{m} \text{tr}(\mathbf{R}) = \mathcal{O}(1)$ .

Note that the pilots energy  $T_p \rho_p$  controls the quality of the estimation. In fact, as  $T_p \rho_p \rightarrow \infty$ ,  $\hat{\mathbf{A}} \rightarrow \mathbf{A}$  which corresponds to the perfect CSI case. By invoking the orthogonality principle of the LMMSE estimator, it can be shown that the  $k^{\text{th}}$  column of the estimation error matrix  $\Delta = \hat{\mathbf{A}} - \mathbf{A}$  follows the distribution  $\mathcal{N}(\mathbf{0}, \mathbf{R}_\Delta)$  with a covariance matrix  $\mathbf{R}_\Delta = \mathbf{R} - \mathbf{R}_{\hat{\mathbf{A}}}$ . Also, from the orthogonality principle of the LMMSE, one can show that  $\hat{\mathbf{A}}$  and  $\Delta$  are statistically independent.

### B. Symbol Detection via BRO

Since modern massive MIMO systems are equipped with a large number of antennas, the computational complexity of optimum algorithms, such as the maximum-likelihood (ML) and sphere decoders, increases exponentially as the problem size grows. Many heuristic low-complexity detection algorithms are thus proposed such as zero-forcing (ZF), linear minimum mean square error (LMMSE) and lattice reduction. To obtain a reasonable computational complexity, one popular heuristic that is used in this paper is the so called box-relaxation optimization (BRO) decoder [23], [24], which is a natural convex relaxation of the optimum ML decoder. In this decoder, the discrete set  $\{\pm 1\}^n$  is relaxed to the convex set  $[-1, +1]^n$ , and now the signal can be recovered via efficient convex optimization followed by hard thresholding. The BRO decoder has been shown to outperform conventional decoders such ZF decoder as we will explain in the next sections.

The BRO decoder consists of two steps. The first step involves solving a convex quadratic optimization with linear constraints. The output of this optimization is hard-thresholded in the second step to produce the desired binary solution. Formally, the algorithm produces an estimate  $\hat{\mathbf{x}}^*$  of  $\mathbf{x}_0$  given as

$$\hat{\mathbf{x}} := \arg \min_{-1 \leq \mathbf{x} \leq 1} \frac{1}{n} \|\mathbf{y} - \sqrt{\frac{\rho_d}{n}} \hat{\mathbf{A}} \mathbf{x}\|^2, \quad (4a)$$

$$\mathbf{x}^* := \text{sign}(\hat{\mathbf{x}}), \quad (4b)$$

where  $\|\cdot\|$  denotes the  $\ell_2$ -norm of a vector and the  $\text{sign}(\cdot)$  function returns the sign of its input and acts element-wise on vector inputs.

We consider the following two metrics to evaluate the performance of the BRO decoder:

*Mean Square Error:* This metric is concerned with the evaluation of performance of the first step (estimation step) of the decoder in (4a). Formally, the mean square error (MSE) is defined as

$$\text{MSE} := \frac{1}{n} \|\hat{\mathbf{x}} - \mathbf{x}_0\|^2. \quad (5)$$

*Bit Error Rate:* For the second step (detection step) in (4b), we evaluate the performance of the decoder by the bit error rate (BER), defined as

$$\text{BER} := \frac{1}{n} \sum_{i=1}^n \mathbb{1}_{\{\mathbf{x}_i^* \neq \mathbf{x}_{0,i}\}}, \quad (6)$$

where  $\mathbb{1}_{\{\cdot\}}$  denotes the indicator function.

### III. LARGE SYSTEM ANALYSIS AND POWER OPTIMIZATION

#### A. Large System Error Analysis

In this section, we present the large system analysis of the BRO decoder in (4) in terms of the MSE and BER. Then, these results will be used later to find the optimal power allocation. Before doing so, we need to state some technical assumptions first.

**Assumption 1.** *We assume that the number of transmit and receive antennas  $n$  and  $m$  are growing large to infinity with a fixed ratio  $\frac{m}{n} \rightarrow \beta$ , for a fixed constant  $\beta > \frac{1}{2}$ .*<sup>2</sup>

**Assumption 2.** *We assume that the normalized coherence time, normalized number of pilot symbols and normalized number data symbols are fixed and given as*

$$\begin{aligned}\frac{T}{n} &\rightarrow \tau \in (1, \infty), \\ \frac{T_p}{n} &\rightarrow \tau_p \in [1, \infty),\end{aligned}$$

and

$$\frac{T_d}{n} \rightarrow \tau_d,$$

respectively.

Note that under Assumption 2, the covariance matrix of  $\hat{\mathbf{A}}$  becomes  $\mathbf{R}_{\hat{\mathbf{A}}} = \mathbf{R} \left( \mathbf{R} + \frac{1}{\tau_p \rho_p} \mathbf{I}_m \right)^{-1} \mathbf{R}$ . Define the spectral decomposition of  $\mathbf{R}_{\hat{\mathbf{A}}}$  as  $\mathbf{R}_{\hat{\mathbf{A}}} = \mathbf{U} \Lambda \mathbf{U}^\top$ , where  $\mathbf{U} \in \mathbb{R}^{m \times m}$  is an orthonormal matrix and  $\Lambda \in \mathbb{R}^{m \times m}$  is a diagonal matrix with the eigenvalues of  $\mathbf{R}_{\hat{\mathbf{A}}}$  on its main diagonal. Let  $Q(\cdot)$  denote the  $Q$ -function associated with the standard normal probability density function (pdf). Finally, for a sequence of random variables  $\{\Theta_n\}_{[n=1,2,\dots]}$ , we write  $\Theta_n \xrightarrow{P} \Theta$  to denote convergence in probability towards a constant  $\Theta$  as  $n \rightarrow \infty$ .

**Theorem 1** (MSE of the BRO). *Let MSE denote the mean square error of the BRO decoder in (4), then under Assumption 1 and Assumption 2, it holds*

$$|\text{MSE} - F(\mu_*)| \xrightarrow{P} 0, \quad (7)$$

where  $\mu_*$  is the unique solution to the following scalar optimization problem:

$$\min_{\mu > 0} \max_{\gamma > 0} \frac{1}{2n} \sum_{j=1}^m \frac{\rho_d \lambda_j F(\mu) + \rho_d [\mathbf{R}_\Delta]_{jj} + 1}{\frac{1}{2} + \frac{\lambda_j \sqrt{\rho_d}}{\gamma}} - \frac{\sqrt{\rho_d}}{2} \Upsilon^2(\mu) \gamma, \quad (8)$$

<sup>2</sup>The phase transition at  $\frac{1}{2}$  is the threshold for the BRO to successfully recovers the true signal  $\mathbf{x}_0$ . [27]

and  $F(\mu) := 4\left(Q(\mu) + \frac{\varphi(\mu)}{\mu^2}\right)$ ,  $\Upsilon(\mu) := \frac{1}{\mu}(1 - 2Q(\mu))$ ,  $\varphi(\mu) := \frac{1}{2} - Q(\mu) - \frac{\mu}{\sqrt{2\pi}}e^{-\frac{\mu^2}{2}}$  and  $\lambda_j$  is the  $j^{th}$  eigenvalue of the matrix  $\mathbf{R}_{\hat{A}}$ .

*Proof.* The proof is deferred to Section V.  $\square$

**Remark 1.** Note that the above MSE result holds for  $\mathbf{x}_0$  drawn from any distribution with zero mean and unit variance and not necessarily from a BPSK constellation.

The next theorem presents the asymptotic BER approximation of the BRO decoder.

**Theorem 2** (BER of the BRO). *Let BER denote the bit error rate of the BRO decoder in (4). Then, under the same setting of Theorem 1, it holds that*

$$\left| \text{BER} - Q\left(\frac{\mu_*}{2}\right) \right| \xrightarrow{P} 0. \quad (9)$$

*Proof.* The proof is given in Section V.  $\square$

**Remark 2.** Although the CGMT requires an asymptotic regime in which  $m, n \rightarrow \infty$ , the approximations are already accurate for small values of  $m, n$ , for example see Fig. 5.

### B. Optimal Power Allocation

In this subsection, we will use the previous asymptotic approximations of the MSE and BER to find the optimum power allocation between pilot and data symbols to minimize the MSE or BER. For a fixed  $\tau_p$  and  $\tau$ , the power allocation optimization can be cast as

$$\alpha_*^{\text{MSE}} := \arg \min_{0 \leq \alpha \leq 1} \text{MSE},$$

where MSE is the asymptotic MSE expression in (7). Similarly, we have

$$\alpha_*^{\text{BER}} := \arg \min_{0 \leq \alpha \leq 1} \text{BER}.$$

However, based on (9), since minimizing the  $Q$ -function amounts to maximizing its argument, we have

$$\alpha_*^{\text{BER}} := \arg \max_{0 \leq \alpha \leq 1} \mu_*.$$

Fig. 1 illustrates the optimized data power ratio  $\alpha_*$  versus the correlation coefficient  $r$  for a total average power of  $\rho = 10$  dB, where we used the exponential correlation model for  $\mathbf{R}$  which is defined as [38], [39]

$$\mathbf{R}(r) = r^{|i-j|^2}, r \in [0, 1], i, j = 1, 2, \dots, m. \quad (10)$$

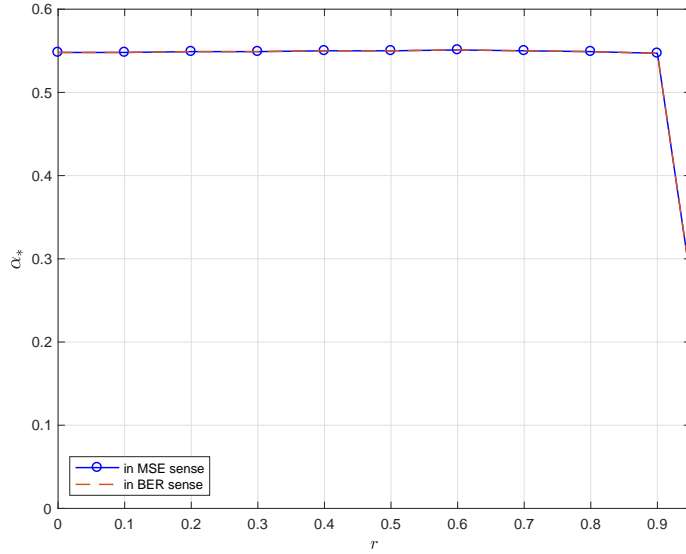


Fig. 1: Optimal data power ratio  $\alpha_*$  v.s. correlation coefficient  $r$ , with  $\beta = 1.5, n = 500, \rho = 10 \text{ dB}, T = 1000, T_p = n$ .

From this figure, we can see that  $\alpha_*^{\text{MSE}} = \alpha_*^{\text{BER}}$ . This indicates that optimizing the MSE is equivalent to optimizing the BER for the considered BRO decoder. Similar observation was found in [16]. In Fig. 2, we find the power allocation for low total average SNR of  $\rho = -10 \text{ dB}$ .

As another illustration, in Fig. 3, we plot the asymptotic approximations of the MSE and BER in Theorem 1 and Theorem 2 respectively as a function of the data power ratio  $\alpha$ . From both figures, we can see that  $\alpha_* \approx 0.55$  for  $r \in [0, 0.9]$ .

#### IV. NUMERICAL RESULTS

To validate our theoretical predictions of the MSE as given by Theorem 1 and BER as stated in Theorem 2, we consider the exponential correlation model for  $\mathbf{R}$  defined in (10). Fig. 4 shows the MSE performance of the BRO decoder for different values of the average expected power  $\rho$  and different values of the correlation coefficient  $r$ . Monte Carlo Simulations are used to validate the theoretical prediction of Theorem 1. Comparing the simulation results to the asymptotic MSE prediction of Theorem 1 shows the close match between the two. Fig. 5 also shows the close match between simulation results and the asymptotic BER prediction of Theorem 2. We used  $n = 400, \beta = 1.5, \alpha = 0.5, T = 1000, T_p = n$ , and the data are averaged over 100 independent Monte-Carlo iterations.

**Double Descent:** In Fig. 6, we plot the MSE and BER vs the ratio of the number of Rx antennas to the number of Tx antennas  $\beta := \frac{m}{n}$ . From the figures, we can see that the BRO decoder clearly out

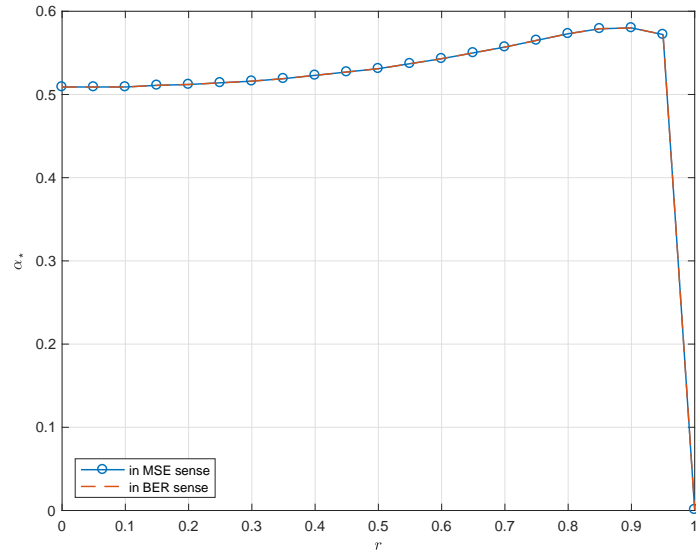


Fig. 2: Optimal data power ratio  $\alpha_*$  v.s. correlation coefficient  $r$ , with  $\beta = 1.5, n = 500, \rho = -10$  dB,  $T = 1000, T_p = n$ .

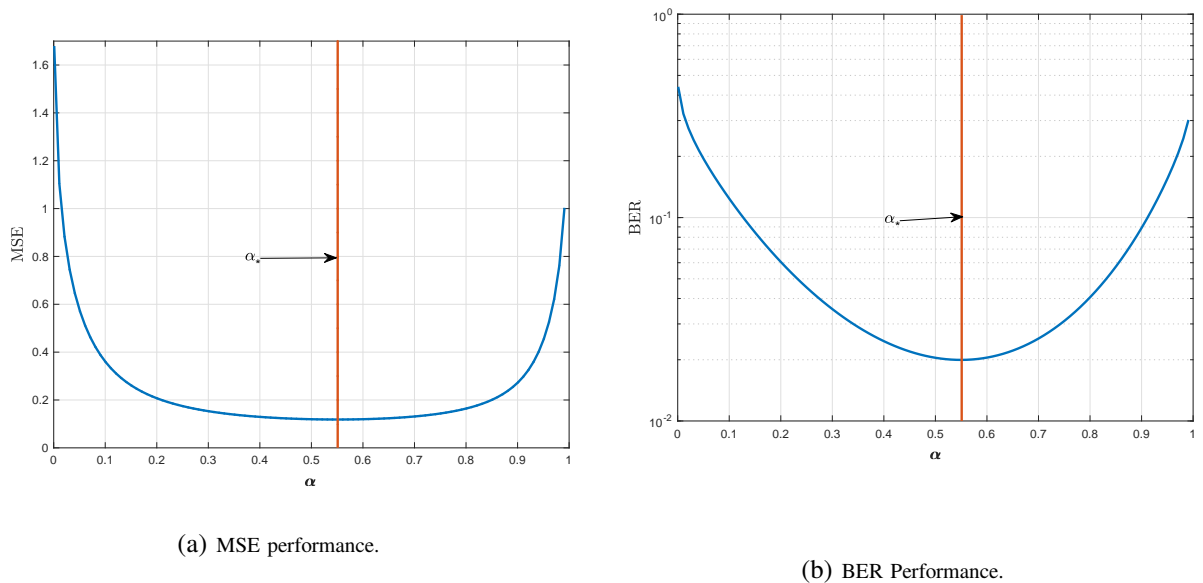


Fig. 3: Performance of BRO decoder vs  $\alpha$ , with  $\beta = 1.5, n = 500, r = 0.4, \rho = 10$  dB,  $T = 1000, T_p = n$ .

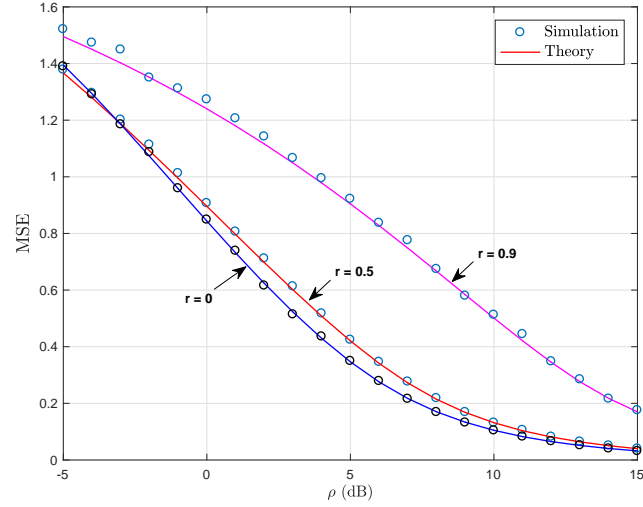


Fig. 4: MSE performance of the BRO decoder.

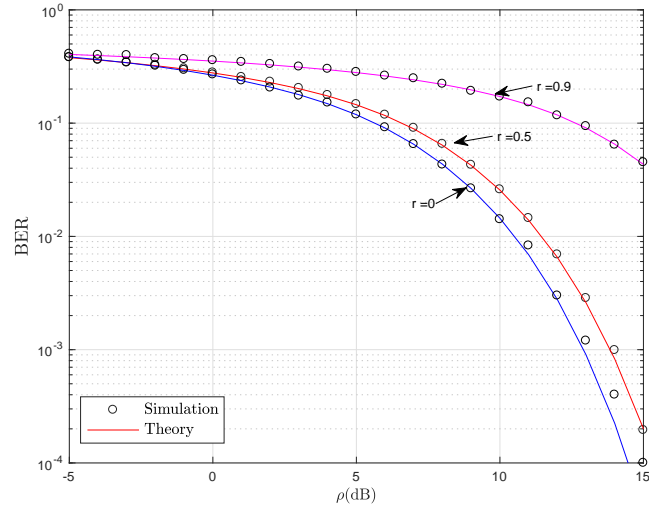


Fig. 5: BER performance of the BRO decoder.

performs the conventional Least Squares (LS) decoder (also known as the Zero-Forcing (ZF) decoder). Note that the MSE and BER of the **LS** detector first decrease for small values of  $\beta$ , then, it increases until it reaches a peak known as the interpolation threshold (at  $\beta = 1$ ) [40]. After the peak, both metrics decrease monotonically as a function of  $\beta$ . This behavior is known as the *double descent* phenomenon [40], [41]. These figures show the important role played by the box-constraint of the BRO decoder in

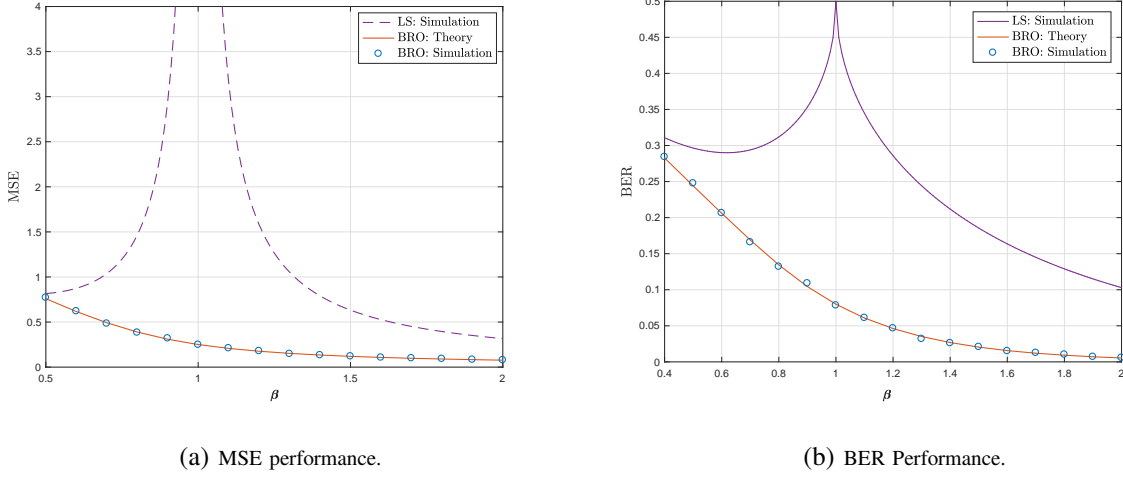


Fig. 6: Performance of BRO decoder vs  $\beta$ , with  $n = 400, r = 0.2, \alpha = 0.5, \rho = 10$  dB,  $T = 1000, T_p = n$ .

reducing MSE/BER and in the mitigation of the double descent phenomenon. This is expected since the box constraint of the BRO can be thought of as an  $\ell_\infty$ -norm regularizer. The authors of [31], [40], [41] showed that optimal regularization can mitigate the double descent effect.

## V. PROOF OUTLINE

In this section, we use the CGMT framework [26] to give a proof outline of Theorems 1 and 2. For the reader convenience, the CGMT is summarized next.

### A. Technical Tool: Convex Gaussian Min-max Theorem

The CGMT allows us to replace the analysis of a generally hard optimization problem with a simplified auxiliary optimization problem. In this subsection, we recall the statement of the CGMT, and we refer the interested reader to [26], [27] for the complete technical details. In order to summarize the essential ideas, we consider the following two Gaussian processes:

$$X_{\mathbf{w}, \mathbf{u}} := \mathbf{u}^\top \mathbf{G} \mathbf{w} + \psi(\mathbf{w}, \mathbf{u}),$$

$$Y_{\mathbf{w}, \mathbf{u}} := \|\mathbf{w}\| \mathbf{g}^\top \mathbf{u} + \|\mathbf{u}\|_2 \mathbf{h}^\top \mathbf{w} + \psi(\mathbf{w}, \mathbf{u}),$$

where  $\mathbf{G} \in \mathbb{R}^{m \times n}$ ,  $\mathbf{g} \in \mathbb{R}^m$ , and  $\mathbf{h} \in \mathbb{R}^n$  are all assumed to have iid standard Gaussian entries. Further let  $\mathcal{S}_w \subset \mathbb{R}^n$ , and  $\mathcal{S}_u \subset \mathbb{R}^m$  be convex and compact sets, and  $\psi : \mathbb{R}^n \times \mathbb{R}^m \rightarrow \mathbb{R}$  is convex-concave continuous on  $\mathcal{S}_w \times \mathcal{S}_u$ , possibly random but independent of  $\mathbf{G}$ . For these two processes, define the

following random min-max optimization problems, which we refer to as the primary optimization (PO) problem and the auxiliary optimization (AO):

$$\Phi^n(\mathbf{G}) := \min_{\mathbf{w} \in \mathcal{S}_w} \max_{\mathbf{u} \in \mathcal{S}_u} X_{\mathbf{w}, \mathbf{u}}, \quad (11a)$$

$$\phi^n(\mathbf{g}, \mathbf{h}) := \min_{\mathbf{w} \in \mathcal{S}_w} \max_{\mathbf{u} \in \mathcal{S}_u} Y_{\mathbf{w}, \mathbf{u}}. \quad (11b)$$

Then, the CGMT relates the above problems as shown in the next theorem, the proof of which can be found in [26].

**Theorem 3** (CGMT [26]). *Let  $\mathcal{S}$  be any arbitrary open subset of  $\mathcal{S}_w$ , and  $\mathcal{S}^c = \mathcal{S}_w \setminus \mathcal{S}$ . Denote  $\phi_{\mathcal{S}^c}^n(\mathbf{g}, \mathbf{h})$  the optimal cost of the optimization in (11b) when the minimization over  $\mathbf{w}$  is constrained over  $\mathbf{w} \in \mathcal{S}^c$ . Suppose that there exist constants  $\bar{\phi}$  and  $\bar{\phi}_{\mathcal{S}^c}$  such that (i)  $\phi^n(\mathbf{g}, \mathbf{h}) \rightarrow \bar{\phi}$  in probability, (ii)  $\phi_{\mathcal{S}^c}^n(\mathbf{g}, \mathbf{h}) \rightarrow \bar{\phi}_{\mathcal{S}^c}$  in probability, and (iii)  $\bar{\phi} < \bar{\phi}_{\mathcal{S}^c}$ . Then,  $\lim_{n \rightarrow \infty} \mathbb{P}[\mathbf{w}_\Phi \in \mathcal{S}] = 1$ , where  $\mathbf{w}_\Phi$  is a minimizer of (11a).*

It is not difficult to see that the conditions (i), (ii) and (iii) regarding the optimal cost of the AO imply that its solution  $\mathbf{w}_\phi$  satisfies:  $\lim_{n \rightarrow \infty} \mathbb{P}[\mathbf{w}_\phi \in \mathcal{S}] = 1$ . The non-trivial and powerful part of the CGMT is that the same conclusion holds true for the optimal solution  $\mathbf{w}_\Phi$  of the PO [27].

Having introduced the CGMT, we will proceed by providing an outline of the proof of Theorem 1 and Theorem 2. The steps of the proof are presented in the following subsections.

### B. PO and AO Identification

For notational convenience, we consider the error vector  $\mathbf{e} := \mathbf{x} - \mathbf{x}_0$ , then the problem in (4) can be reformulated as

$$\hat{\mathbf{e}} = \arg \min_{-2 \leq \mathbf{e} \leq 0} \frac{1}{n} \left\| \sqrt{\frac{\rho_d}{n}} \hat{\mathbf{A}} \mathbf{e} + \sqrt{\frac{\rho_d}{n}} \Delta \mathbf{x}_0 - \mathbf{z} \right\|^2. \quad (12)$$

Without loss of generality, we assume for the analysis that  $\mathbf{x}_0 = \mathbf{1}_n = [1, 1, \dots, 1]^\top$ . Then,  $\text{BER} = \frac{1}{n} \sum_{i=1}^n \mathbb{1}_{\{\hat{x}_i \leq 0\}}$ . Next, note that  $\hat{\mathbf{A}}$  can be written as  $\hat{\mathbf{A}} = \mathbf{R}_{\hat{\mathbf{A}}}^{1/2} \mathbf{B}$ , with  $\mathbf{B}$  being a Gaussian matrix with iid standard normal entries and  $\mathbf{R}_{\hat{\mathbf{A}}}$  is the covariance matrix of  $\hat{\mathbf{A}}$  as defined before. Thus, we have

$$\hat{\mathbf{e}} = \arg \min_{-2 \leq \mathbf{e} \leq 0} \frac{1}{n} \left\| \sqrt{\frac{\rho_d}{n}} \mathbf{R}_{\hat{\mathbf{A}}}^{1/2} \mathbf{B} \mathbf{e} + \sqrt{\frac{\rho_d}{n}} \Delta \mathbf{x}_0 - \mathbf{z} \right\|^2, \quad (13)$$

Since the Gaussian distribution is invariant under orthogonal transformations, and recalling that the spectral decomposition of  $\mathbf{R}_{\hat{\mathbf{A}}}$  is  $\mathbf{R}_{\hat{\mathbf{A}}} = \mathbf{U} \Lambda \mathbf{U}^\top$ , we have

$$\hat{\mathbf{e}} = \arg \min_{-2 \leq \mathbf{e} \leq 0} \frac{1}{n} \left\| \sqrt{\frac{\rho_d}{n}} \Lambda^{1/2} \mathbf{B} \mathbf{e} + \sqrt{\frac{\rho_d}{n}} \Delta \mathbf{x}_0 - \mathbf{z} \right\|^2. \quad (14)$$

The loss function can be expressed in its dual form through the Fenchel's conjugate as

$$\left\| \sqrt{\frac{\rho_d}{n}} (\Lambda^{1/2} \mathbf{B} \mathbf{e} + \Delta \mathbf{x}_0) - \mathbf{z} \right\|^2 = \max_{\tilde{\mathbf{u}}} \tilde{\mathbf{u}}^\top \left( \sqrt{\frac{\rho_d}{n}} (\Lambda^{1/2} \mathbf{B} \mathbf{e} + \Delta \mathbf{x}_0) - \mathbf{z} \right) - \frac{\|\tilde{\mathbf{u}}\|^2}{4}.$$

Then, (14) becomes <sup>3</sup>

$$\mathfrak{D}_1^n : \frac{1}{n} \min_{-2 \leq \mathbf{e} \leq 0} \max_{\tilde{\mathbf{u}}} \sqrt{\frac{\rho_d}{n}} \tilde{\mathbf{u}}^\top \Lambda^{1/2} \mathbf{B} \mathbf{e} + \sqrt{\frac{\rho_d}{n}} \tilde{\mathbf{u}}^\top \Delta \mathbf{x}_0 - \frac{\|\tilde{\mathbf{u}}\|^2}{4}. \quad (15)$$

Defining  $\mathbf{u} := \frac{1}{\sqrt{n}} \Lambda^{1/2} \tilde{\mathbf{u}}$  yields

$$\mathfrak{D}_2^n : \min_{-2 \leq \mathbf{e} \leq 0} \max_{\mathbf{u} \in \mathcal{S}_u} \frac{\sqrt{\rho_d}}{n} \mathbf{u}^\top \mathbf{B} \mathbf{e} + \frac{\sqrt{\rho_d}}{n} \mathbf{u}^\top \Lambda^{-1/2} \Delta \mathbf{x}_0 - \frac{1}{\sqrt{n}} \mathbf{u}^\top \Lambda^{-1/2} \mathbf{z} - \frac{1}{4} \mathbf{u}^\top \Lambda^{-1} \mathbf{u}, \quad (16)$$

where  $\mathcal{S}_u = \{\mathbf{u} \in \mathbb{R}^m : \|\mathbf{u}\| \leq C_u\}$ , for some fixed constant  $C_u > 0$  that is independent of  $n$ . The above optimization is in a PO form, and its *corresponding AO* is

$$\tilde{\mathfrak{D}}_1^n : \min_{-2 \leq \mathbf{e} \leq 0} \max_{\mathbf{u} \in \mathcal{S}_u} \frac{\sqrt{\rho_d}}{n} \|\mathbf{e}\| \mathbf{g}^\top \mathbf{u} - \frac{\sqrt{\rho_d}}{n} \|\mathbf{u}\| \mathbf{h}^\top \mathbf{e} + \frac{\sqrt{\rho_d}}{n} \mathbf{u}^\top \Lambda^{-1/2} \Delta \mathbf{x}_0 - \frac{1}{\sqrt{n}} \mathbf{u}^\top \Lambda^{-1/2} \mathbf{z} - \frac{1}{4} \mathbf{u}^\top \Lambda^{-1} \mathbf{u}, \quad (17)$$

where  $\mathbf{g} \sim \mathcal{N}(\mathbf{0}, \mathbf{I}_m)$  and  $\mathbf{h} \sim \mathcal{N}(\mathbf{0}, \mathbf{I}_n)$  are independent vectors.

Fixing the norm of the normalized error vector  $\frac{\mathbf{e}}{\sqrt{n}}$  to  $\xi := \frac{\|\mathbf{e}\|}{\sqrt{n}}$ , we get

$$\begin{aligned} \tilde{\mathfrak{D}}_2^n : \min_{\xi \geq 0} \max_{\mathbf{u} \in \mathcal{S}_u} & \xi \sqrt{\frac{\rho_d}{n}} \mathbf{g}^\top \mathbf{u} + \frac{\sqrt{\rho_d}}{n} \mathbf{u}^\top \Lambda^{-1/2} \Delta \mathbf{x}_0 \\ & - \frac{1}{\sqrt{n}} \mathbf{u}^\top \Lambda^{-1/2} \mathbf{z} - \frac{1}{4} \mathbf{u}^\top \Lambda^{-1} \mathbf{u} + \sqrt{\rho_d} \|\mathbf{u}\| \min_{\substack{\|\mathbf{e}\| = \sqrt{n}\xi \\ -2 \leq \mathbf{e} \leq 0}} -\frac{1}{n} \mathbf{h}^\top \mathbf{e}. \end{aligned} \quad (18)$$

Now, applying Lemma 1, and under the condition,  $\xi^2 \leq \frac{4}{n} \sum_{i=1}^n \mathbb{1}_{\{h_i < 0\}}$ , we have

$$\hat{\Upsilon}(\xi) := \min_{\substack{\|\mathbf{e}\| = \sqrt{n}\xi \\ -2 \leq \mathbf{e} \leq 0}} -\frac{1}{n} \mathbf{h}^\top \mathbf{e} \quad (19)$$

$$= \frac{2}{n} \left[ \sum_{i=1}^n |h_i| \mathbb{1}_{\{h_i \leq -\hat{\mu}(\xi)\}} + \sum_{i=1}^n \frac{|h_i|^2}{\hat{\mu}(\xi)} \mathbb{1}_{\{-\hat{\mu}(\xi) < h_i < 0\}} \right], \quad (20)$$

where  $\hat{\mu}(\xi)$  verifies

$$\frac{4}{n} \sum_{i=1}^n \mathbb{1}_{\{h_i \leq -\hat{\mu}(\xi)\}} + \frac{4}{\hat{\mu}(\xi)^2 n} \sum_{i=1}^n |h_i|^2 \mathbb{1}_{\{-\hat{\mu}(\xi) < h_i < 0\}} = \xi^2. \quad (21)$$

In the limit as  $n \rightarrow \infty$ , equation (21) converges to

$$4 \left( Q(\mu(\xi)) + \frac{\varphi(\mu(\xi))}{\mu^2(\xi)} \right) = \xi^2, \quad (22)$$

<sup>3</sup>One technical requirement of the CGMT is the compactness of the feasibility set  $\mathcal{S}_u$  which can be handled by noting that the optimal  $\mathbf{e}_*$  is bounded, and since  $\tilde{\mathbf{u}}_* = 2\sqrt{\frac{\rho_d}{n}}(\Lambda^{1/2} \mathbf{B} \mathbf{e}_* + \Delta \mathbf{x}_0) - 2\mathbf{z}$ , then there exists a constant  $C_{\tilde{\mathbf{u}}} > 0$  such that  $\|\tilde{\mathbf{u}}_*\| \leq C_{\tilde{\mathbf{u}}}$  with probability going to 1.

with  $\varphi(t) := \frac{1}{2} - Q(t) - \frac{x}{\sqrt{2\pi}}e^{-t^2/2}$ , and the following convergence results hold true

$$\hat{\Upsilon}(\xi) - \Upsilon(\mu(\xi)) \xrightarrow{P} 0, \quad (23a)$$

$$\hat{\mu}(\xi) - \mu(\xi) \xrightarrow{P} 0, \quad (23b)$$

with  $\Upsilon(t) := \frac{1}{t}(1 - 2Q(t))$  and  $\mu(\xi)$  is the unique positive solution of the following fixed-point equation

$$\mu(\xi) = 2\sqrt{\frac{\varphi(\mu(\xi))}{\xi^2 - 4Q(\mu(\xi))}}, \quad (24)$$

where (24) is found from (22). For notational simplicity, we will denote  $\mu(\xi)$  by  $\mu$  only. Note that  $\frac{1}{n}\sum_{i=1}^n \mathbb{1}_{\{h_i < 0\}} \xrightarrow{P} \frac{1}{2}$ , then the condition  $\xi^2 \leq \frac{4}{n}\sum_{i=1}^n \mathbb{1}_{\{h_i < 0\}}$  asymptotically becomes  $\xi^2 \leq 2$ . Then, applying Lemma 10 in [26], we have  $\tilde{\mathcal{D}}_2^n - \tilde{\mathcal{D}}_3^n \xrightarrow{P} 0$ , where

$$\begin{aligned} \tilde{\mathcal{D}}_3^n : \min_{0 < \xi \leq \sqrt{2}} \max_{\mathbf{u} \in \mathcal{S}_u} & \xi \sqrt{\frac{\rho_d}{n}} \mathbf{g}^\top \mathbf{u} + \frac{\sqrt{\rho_d}}{n} \mathbf{u}^\top \mathbf{\Lambda}^{-1/2} \mathbf{\Delta} \mathbf{x}_0 \\ & - \frac{1}{\sqrt{n}} \mathbf{u}^\top \mathbf{\Lambda}^{-1/2} \mathbf{z} - \frac{1}{4} \mathbf{u}^\top \mathbf{\Lambda}^{-1} \mathbf{u} - \sqrt{\rho_d} \|\mathbf{u}\| \Upsilon(\mu). \end{aligned} \quad (25)$$

From the identity,  $\|\mathbf{u}\| = \min_{\chi > 0} \frac{\chi}{2} + \frac{\|\mathbf{u}\|^2}{2\chi}$ , we can write

$$\begin{aligned} \tilde{\mathcal{D}}_4^n : \min_{0 < \xi \leq \sqrt{2}} \max_{\substack{\mathbf{u} \in \mathcal{S}_u \\ \chi > 0}} & \frac{1}{\sqrt{n}} \left( \sqrt{\rho_d} \xi \mathbf{g} + \mathbf{\Lambda}^{-1/2} \left( \sqrt{\frac{\rho_d}{n}} \mathbf{\Delta} \mathbf{x}_0 - \mathbf{z} \right) \right)^\top \mathbf{u} \\ & - \frac{\sqrt{\rho_d} \chi}{2} \Upsilon(\mu) - \frac{\sqrt{\rho_d} \Upsilon(\mu) \|\mathbf{u}\|^2}{2\chi} - \frac{1}{4} \mathbf{u}^\top \mathbf{\Lambda}^{-1} \mathbf{u}. \end{aligned} \quad (26)$$

Let  $\tilde{\mathbf{g}} := \sqrt{\rho_d} \xi \mathbf{g} + \mathbf{\Lambda}^{-1/2} \left( \sqrt{\frac{\rho_d}{n}} \mathbf{\Delta} \mathbf{x}_0 - \mathbf{z} \right)$ , and  $\mathbf{\Xi} := \frac{1}{2} \mathbf{\Lambda}^{-1} + \frac{\sqrt{\rho_d}}{\chi} \Upsilon(\mu) \mathbf{I}_m$ , then

$$\tilde{\mathcal{D}}_5^n : \min_{0 < \xi \leq \sqrt{2}} \max_{\substack{\mathbf{u} \in \mathcal{S}_u \\ \chi > 0}} \frac{1}{\sqrt{n}} \tilde{\mathbf{g}}^\top \mathbf{u} - \frac{1}{2} \mathbf{u}^\top \mathbf{\Xi} \mathbf{u} - \frac{\chi \sqrt{\rho_d}}{2} \Upsilon(\mu). \quad (27)$$

The optimal  $\mathbf{u}_*$  can be easily found as  $\mathbf{u}_* = \frac{1}{\sqrt{n}} \mathbf{\Xi}^{-1} \tilde{\mathbf{g}}$ . Thus, the AO can be written as

$$\tilde{\mathcal{D}}_6^n : \min_{0 < \xi \leq \sqrt{2}} \max_{\chi > 0} \frac{1}{2n} \tilde{\mathbf{g}}^\top \mathbf{\Xi}^{-1} \tilde{\mathbf{g}}^\top - \frac{\sqrt{\rho_d} \chi}{2} \Upsilon(\mu). \quad (28)$$

### C. Large System Analysis of the AO

Note that  $\tilde{\mathbf{g}}$  is distributed as  $\mathcal{N}(\mathbf{0}, \mathbf{R}_{\tilde{\mathbf{g}}})$ , with covariance matrix  $\mathbf{R}_{\tilde{\mathbf{g}}} := \mathbb{E}[\tilde{\mathbf{g}} \tilde{\mathbf{g}}^\top]$  that is given by

$$\mathbf{R}_{\tilde{\mathbf{g}}} = \rho_d \xi^2 \mathbf{I}_m + \rho_d \mathbf{R}_\Delta \mathbf{\Lambda}^{-1} + \mathbf{\Lambda}^{-1}.$$

Then, using the trace lemma [42], we get  $\frac{1}{n} \tilde{\mathbf{g}}^\top \mathbf{\Xi}^{-1} \tilde{\mathbf{g}}^\top - \frac{1}{n} \text{tr}(\mathbf{R}_{\tilde{\mathbf{g}}} \mathbf{\Xi}^{-1}) \xrightarrow{P} 0$ . Again using Lemma 10 of [26],  $\tilde{\mathcal{D}}_6^n - \tilde{\mathcal{D}}_7^n \xrightarrow{P} 0$ , where

$$\tilde{\mathcal{D}}_7^n : \min_{0 < \xi \leq \sqrt{2}} \max_{\chi > 0} \frac{1}{2n} \sum_{j=1}^m \frac{\rho_d \lambda_j \xi^2 + \rho_d [\mathbf{R}_\Delta]_{jj} + 1}{\frac{1}{2} + \frac{\sqrt{\rho_d} \lambda_j \Upsilon(\mu)}{\chi}} - \frac{\sqrt{\rho_d}}{2} \Upsilon(\mu) \chi. \quad (29)$$

Performing the change of variable  $\gamma := \frac{\chi}{\Upsilon(\mu)}$ , we have

$$\tilde{\mathcal{D}}_8^n : \min_{0 < \xi \leq \sqrt{2}} \max_{\gamma > 0} \frac{1}{2n} \sum_{j=1}^m \frac{\rho_d \lambda_j \xi^2 + \rho_d [\mathbf{R}_\Delta]_{jj} + 1}{\frac{1}{2} + \frac{\sqrt{\rho_d} \lambda_j}{\gamma}} - \frac{\sqrt{\rho_d}}{2} \Upsilon^2(\mu) \gamma. \quad (30)$$

Using equation (22), we have

$$\xi^2 = F(\mu) := 4 \left( Q(\mu) + \frac{f(\mu)}{\mu^2} \right). \quad (31)$$

One can easily show that  $F(\cdot)$  is a strictly decreasing function on  $(0, \infty)$ , and then using the change of variables rule in [43, page 130], we can make the change of variable  $\xi^2 = F(\mu)$  to get

$$\tilde{\mathcal{D}}_9^n : \min_{\mu > 0} \max_{\gamma > 0} \frac{1}{2n} \sum_{j=1}^m \frac{\rho_d \lambda_j F(\mu) + \rho_d [\mathbf{R}_\Delta]_{jj} + 1}{\frac{1}{2} + \frac{\sqrt{\rho_d} \lambda_j}{\gamma}} - \frac{\sqrt{\rho_d}}{2} \Upsilon^2(\mu) \gamma. \quad (32)$$

One can show that the cost function of  $\tilde{\mathcal{D}}_9^n$  is strictly positive for all  $\gamma > 0$  by checking its second derivative with respect to  $\mu$ . Hence,  $\tilde{\mathcal{D}}_9^n$  has a unique minimizer  $\mu_*$ . This implies that  $\tilde{\mathcal{D}}_8^n$  has a unique minimizer  $\xi_*$ .

#### D. Using the CGMT: Theorem 1 and Theorem 2 Proofs

We start by proving Theorem 1, where we analyze the asymptotic behavior of the MSE of the BRO. Let  $\tilde{\mathbf{e}}$  be the optimal solution to the AO defined as the solution to  $\tilde{\mathcal{D}}_1^n$ . Define  $\hat{\xi}$  as the minimizer of (18). By definition,  $\hat{\xi}^2 = \frac{\|\tilde{\mathbf{e}}\|^2}{n}$ . In the previous section, we have shown that  $\tilde{\mathcal{D}}_1^n - \tilde{\mathcal{D}}_8^n \xrightarrow{P} 0$ , and since  $\tilde{\mathcal{D}}_8^n$  in (30) has a unique minimizer  $\xi_*$ , then  $\hat{\xi} - \xi_* \xrightarrow{P} 0$  which implies that for any  $\varepsilon > 0$ , and with probability approaching 1 (w.p.a.1), we have

$$\tilde{\mathbf{e}} \in \mathcal{S}_{\text{MSE}} := \left\{ \mathbf{s} \in \mathbb{R}^n : \left| \frac{1}{n} \|\mathbf{s}\|^2 - F(\mu_*) \right| < \varepsilon \right\},$$

where  $F(\mu)$  is as defined in (31) and  $\mu_*$  be the optimal solution to  $\tilde{\mathcal{D}}_9^n$ . Then, applying the CGMT yields that  $\hat{\mathbf{e}} \in \mathcal{S}_{\text{MSE}}$  w.p.a.1 as well. This ends the proof of Theorem 1.

For the BER analysis, we start by changing the set  $\mathcal{S}_{\text{MSE}}$  to the following:

$$\mathcal{S}_{\text{BER}} := \left\{ \mathbf{s} \in \mathbb{R}^n : \left| \frac{1}{n} \sum_{i=1}^n \mathbb{1}_{\{s_i \leq -1\}} - Q\left(\frac{\mu_*}{2}\right) \right| < \varepsilon \right\}.$$

Using the expression of  $\tilde{\mathbf{e}}$  in (34), we can show that

$$\frac{1}{n} \sum_{i=1}^n \mathbb{1}_{\{\tilde{e}_i \leq -1\}} = \frac{1}{n} \sum_{i=1}^n \mathbb{1}_{\{h_i \leq -\hat{\mu}\}} + \frac{1}{n} \sum_{i=1}^n \mathbb{1}_{\{-\hat{\mu} < h_i \leq -\frac{\hat{\mu}}{2}\}}.$$

Then, the right hand side (RHS) of the above equation converges as  $|\text{RHS} - Q\left(\frac{\mu_*}{2}\right)| \xrightarrow{P} 0$ . Therefore,  $\tilde{\mathbf{e}} \in \mathcal{S}_{\text{BER}}$  w.p.a.1.<sup>4</sup> Then, by the CGMT,  $\hat{\mathbf{e}} \in \mathcal{S}_{\text{BER}}$  with probability approaching 1, thus concluding the proof of Theorem 2.

<sup>4</sup>The indicator function  $\mathbb{1}_{\{\tilde{e}_i \leq -1\}}$  is not Lipschitz, so the CGMT cannot be directly applied. However, as discussed in [27, Lemma A.4], this function can be appropriately approximated with Lipschitz functions.

## VI. CONCLUSION

In this work, we derived precise characterization of the asymptotic behavior of the BRO decoder under the assumptions of imperfect CSI and receiver-side correlation. We used the MSE and BER as performance metrics of the decoder. Then, we derived the optimal power allocation between pilot and data symbols using the presented asymptotic results. Simulation results validate our theoretical analysis even for small dimensions of the problem. They also show that the BRO decoder can mitigate the double descent effect encountered with other conventional decoders such as the ZF decoder. For simplicity of the analysis, BPSK signals are used but our results can be extended to higher order modulation schemes such as  $M$ -PAM and is left for future work. Possible future work includes studying the fully correlated MIMO systems (Kronecker correlation), and analyzing the regularized version of the BRO decoder.

## ACKNOWLEDGMENT

This work was supported by the University of Ha'il, Saudi Arabia.

## APPENDIX

**Lemma 1** ([33]). *Let  $\mathbf{h} \in \mathbb{R}^n$  and let  $a$  and  $\xi$  be strictly positive constants such as*

$$\xi^2 \leq a^2 \left( \frac{1}{n} \sum_{i=1}^n \mathbb{1}_{\{h_i < 0\}} \right). \quad (33)$$

*Then,*

$$\begin{aligned} \min_{\substack{\|\mathbf{e}\| = \sqrt{n}\xi \\ -a \leq \mathbf{e} \leq 0}} -\frac{1}{n} \mathbf{h}^\top \mathbf{e} = \\ -\frac{a}{n} \sum_{i=1}^n |h_i| \mathbb{1}_{\{h_i \leq -\mu\}} - \frac{a}{\mu n} \sum_{i=1}^n |h_i|^2 \mathbb{1}_{\{-\mu < h_i < 0\}}, \end{aligned}$$

*where  $\mu$  satisfies*

$$\frac{a^2}{n} \left( \sum_{i=1}^n \mathbb{1}_{\{h_i \leq -\mu\}} + \frac{1}{\mu^2} \sum_{i=1}^n |h_i|^2 \mathbb{1}_{\{-\mu < h_i < 0\}} \right) = \xi^2.$$

*The corresponding optimal  $\mathbf{e}^*$  is given by*

$$e_i^* = \begin{cases} 0, & \text{if } h_i \geq 0 \\ \frac{a}{\mu} h_i, & \text{if } -\mu < h_i < 0 \\ -a, & \text{if } h_i \leq -\mu. \end{cases} \quad (34)$$

*Proof.* See [33]. □

## REFERENCES

- [1] Thomas L Marzetta, "Noncooperative cellular wireless with unlimited numbers of base station antennas," *IEEE transactions on wireless communications*, vol. 9, no. 11, pp. 3590–3600, 2010.
- [2] Jakob Hoydis, Stephan Ten Brink, and Mérouane Debbah, "Massive mimo in the ul/dl of cellular networks: How many antennas do we need?," *IEEE Journal on selected Areas in Communications*, vol. 31, no. 2, pp. 160–171, 2013.
- [3] Erik G Larsson, Ove Edfors, Fredrik Tufvesson, and Thomas L Marzetta, "Massive mimo for next generation wireless systems," *IEEE communications magazine*, vol. 52, no. 2, pp. 186–195, 2014.
- [4] Lu Lu, Geoffrey Ye Li, A Lee Swindlehurst, Alexei Ashikhmin, and Rui Zhang, "An overview of massive mimo: Benefits and challenges," *IEEE journal of selected topics in signal processing*, vol. 8, no. 5, pp. 742–758, 2014.
- [5] Hien Quoc Ngo, Erik G Larsson, and Thomas L Marzetta, "Energy and spectral efficiency of very large multiuser mimo systems," *IEEE Transactions on Communications*, vol. 61, no. 4, pp. 1436–1449, 2013.
- [6] Ekram Hossain, Mehdi Rasti, Hina Tabassum, and Amr Abdelnasser, "Evolution toward 5g multi-tier cellular wireless networks: An interference management perspective," *IEEE Wireless Communications*, vol. 21, no. 3, pp. 118–127, 2014.
- [7] VK Varma Gottumukkala and Hlaing Minn, "Optimal pilot power allocation for ofdm systems with transmitter and receiver iq imbalances," in *GLOBECOM 2009-2009 IEEE Global Telecommunications Conference*. IEEE, 2009, pp. 1–5.
- [8] Arun P Kannu and Philip Schniter, "Capacity analysis of mmse pilot-aided transmission for doubly selective channels," in *IEEE 6th Workshop on Signal Processing Advances in Wireless Communications, 2005*. IEEE, 2005, pp. 801–805.
- [9] Babak Hassibi and Bertrand M Hochwald, "How much training is needed in multiple-antenna wireless links?," *IEEE Transactions on Information Theory*, vol. 49, no. 4, pp. 951–963, 2003.
- [10] Hieu Trong Dao and Sungwan Kim, "Pilot power allocation for maximising the sum rate in massive mimo systems," *IET Communications*, vol. 12, no. 11, pp. 1367–1372, 2018.
- [11] Yasong Zhu, Hairong Wang, and Chen Liu, "Uplink pilot-to-data power ratio design based on user joint optimization algorithm in multi-cell massive mimo system," in *2018 IEEE 18th International Conference on Communication Technology (ICCT)*. IEEE, 2018, pp. 396–401.
- [12] Songtao Lu and Zhengdao Wang, "Training optimization and performance of single cell uplink system with massive-antennas base station," *IEEE Transactions on Communications*, vol. 67, no. 2, pp. 1570–1585, 2018.
- [13] Tarig Ballal, Mohamed A Suliman, Ayed M Alrashdi, and Tareq Y Al-Naffouri, "Optimum pilot and data energy allocation for bpsk transmission over massive mimo systems," in *2019 IEEE Wireless Communications and Networking Conference (WCNC)*. IEEE, 2019, pp. 1–6.
- [14] Peiyue Zhao, Gábor Fodor, György Dán, and Miklós Telek, "A game theoretic approach to setting the pilot power ratio in multi-user mimo systems," *IEEE Transactions on Communications*, vol. 66, no. 3, pp. 999–1012, 2017.
- [15] Kezhi Wang, Yunfei Chen, Mohamed-Slim Alouini, and Feng Xu, "Ber and optimal power allocation for amplify-and-forward relaying using pilot-aided maximum likelihood estimation," *IEEE Transactions on Communications*, vol. 62, no. 10, pp. 3462–3475, 2014.
- [16] Ayed Alrashdi, Abla Kammoun, Ali H Muqabel, and Tareq Y Al-Naffouri, "Optimum m-pam transmission for massive mimo systems with channel uncertainty," *arXiv preprint arXiv:2008.06993*, 2020.
- [17] Ayed M Alrashdi, Ismail Ben Atitallah, Tarig Ballal, Christos Thrampoulidis, Anas Chaaban, and Tareq Y Al-Naffouri, "Optimum training for mimo bpsk transmission," in *2018 IEEE 19th International Workshop on Signal Processing Advances in Wireless Communications (SPAWC)*. IEEE, 2018, pp. 1–5.
- [18] Emil Björnson, Jakob Hoydis, and Luca Sanguinetti, "Massive mimo networks: Spectral, energy, and hardware efficiency," *Foundations and Trends in Signal Processing*, vol. 11, no. 3-4, pp. 154–655, 2017.

- [19] Sebastian Wagner, Romain Couillet, Mérouane Debbah, and Dirk TM Slock, “Large system analysis of linear precoding in correlated miso broadcast channels under limited feedback,” *IEEE transactions on information theory*, vol. 58, no. 7, pp. 4509–4537, 2012.
- [20] Rusdha Muharar, “Optimal power allocation and training duration for uplink multiuser massive mimo systems with mmse receivers,” *IEEE Access*, vol. 8, pp. 23378–23390, 2020.
- [21] Ikram Boukhedimi, Abla Kammoun, and Mohamed-Slim Alouini, “Lmmse receivers in uplink massive mimo systems with correlated rician fading,” *IEEE Transactions on Communications*, vol. 67, no. 1, pp. 230–243, 2018.
- [22] Hei Victor Cheng, Emil Björnson, and Erik G Larsson, “Optimal pilot and payload power control in single-cell massive mimo systems,” *IEEE Transactions on Signal Processing*, vol. 65, no. 9, pp. 2363–2378, 2016.
- [23] Peng Hui Tan, Lars K Rasmussen, and Teng J Lim, “Constrained maximum-likelihood detection in cdma,” *IEEE Transactions on Communications*, vol. 49, no. 1, pp. 142–153, 2001.
- [24] Aylin Yener, Roy D Yates, and Sennur Ulukus, “Cdma multiuser detection: A nonlinear programming approach,” *IEEE Transactions on Communications*, vol. 50, no. 6, pp. 1016–1024, 2002.
- [25] Christos Thrampoulidis, Ehsan Abbasi, Weiyu Xu, and Babak Hassibi, “Ber analysis of the box relaxation for bpsk signal recovery,” in *2016 IEEE International Conference on Acoustics, Speech and Signal Processing (ICASSP)*. IEEE, 2016, pp. 3776–3780.
- [26] Christos Thrampoulidis, Ehsan Abbasi, and Babak Hassibi, “Precise error analysis of regularized  $m$ -estimators in high dimensions,” *IEEE Transactions on Information Theory*, vol. 64, no. 8, pp. 5592–5628, 2018.
- [27] Christos Thrampoulidis, Weiyu Xu, and Babak Hassibi, “Symbol error rate performance of box-relaxation decoders in massive mimo,” *IEEE Transactions on Signal Processing*, vol. 66, no. 13, pp. 3377–3392, 2018.
- [28] Ayed M Alrashdi, Ismail Ben Atitallah, Tareq Y Al-Naffouri, and Mohamed-Slim Alouini, “Precise performance analysis of the lasso under matrix uncertainties,” in *2017 IEEE Global Conference on Signal and Information Processing (GlobalSIP)*. IEEE, 2017, pp. 1290–1294.
- [29] Ismail Ben Atitallah, Christos Thrampoulidis, Abla Kammoun, Tareq Y Al-Naffouri, Mohamed-Slim Alouini, and Babak Hassibi, “The box-lasso with application to gssk modulation in massive mimo systems,” in *2017 IEEE International Symposium on Information Theory (ISIT)*. IEEE, 2017, pp. 1082–1086.
- [30] Ayed M Alrashdi, Ismail Ben Atitallah, and Tareq Y Al-Naffouri, “Precise performance analysis of the box-elastic net under matrix uncertainties,” *IEEE Signal Processing Letters*, vol. 26, no. 5, pp. 655–659, 2019.
- [31] Oussama Dhifallah and Yue M Lu, “A precise performance analysis of learning with random features,” *arXiv preprint arXiv:2008.11904*, 2020.
- [32] Ryo Hayakawa and Kazunori Hayashi, “Asymptotic performance of discrete-valued vector reconstruction via box-constrained optimization with sum of  $\ell_1$  regularizers,” *IEEE Transactions on Signal Processing*, vol. 68, pp. 4320–4335, 2020.
- [33] Ayed M Alrashdi, Houssem Sifaou, Abla Kammoun, Mohamed-Slim Alouini, and Tareq Y Al-Naffouri, “Box-relaxation for bpsk recovery in massive mimo: A precise analysis under correlated channels,” in *ICC 2020-2020 IEEE International Conference on Communications (ICC)*. IEEE, 2020, pp. 1–6.
- [34] Ayed M Alrashdi, Houssem Sifaou, Abla Kammoun, Mohamed-Slim Alouini, and Tareq Y Al-Naffouri, “Precise error analysis of the lasso under correlated designs,” *arXiv preprint arXiv:2008.13033*, 2020.
- [35] Ansuman Adhikary, Junyoung Nam, Jae-Young Ahn, and Giuseppe Caire, “Joint spatial division and multiplexing—the large-scale array regime,” *IEEE transactions on information theory*, vol. 59, no. 10, pp. 6441–6463, 2013.
- [36] Giuseppa Alfano, Antonia M Tulino, Angel Lozano, and Sergio Verdú, “Capacity of mimo channels with one-sided

correlation,” in *Eighth IEEE International Symposium on Spread Spectrum Techniques and Applications-Programme and Book of Abstracts (IEEE Cat. No. 04TH8738)*. IEEE, 2004, pp. 515–519.

[37] Steven M Kay, *Fundamentals of statistical signal processing*, Prentice Hall PTR, 1993.

[38] Hyundong Shin, Moe Z Win, Jae Hong Lee, and Marco Chiani, “On the capacity of doubly correlated mimo channels,” *IEEE Transactions on Wireless Communications*, vol. 5, no. 8, pp. 2253–2265, 2006.

[39] Sergey L Loyka, “Channel capacity of mimo architecture using the exponential correlation matrix,” *IEEE Communications letters*, vol. 5, no. 9, pp. 369–371, 2001.

[40] Mikhail Belkin, Daniel Hsu, Siyuan Ma, and Soumik Mandal, “Reconciling modern machine-learning practice and the classical bias–variance trade-off,” *Proceedings of the National Academy of Sciences*, vol. 116, no. 32, pp. 15849–15854, 2019.

[41] Mikhail Belkin, Siyuan Ma, and Soumik Mandal, “To understand deep learning we need to understand kernel learning,” *arXiv preprint arXiv:1802.01396*, 2018.

[42] T. Couillet and M. Debbah, *Random Matrix Methods for Wireless Communications*, U.K., Cambridge: Cambridge Univ. Press, 2011.

[43] S. Boyd and L. Vandenberghe, *Convex Optimization*, Cambridge University Press, 2003.